

STUDY OF PRIMARY CONTACT IN PROCESS OF FACE MILLING

T. Czánová, J. Pilc, M. Szigety, R. Bobrovsky

Summary

The article deals with the mathematical model of the primary contact of a milling tool in face milling. When designing the mathematical model, there were taken into consideration positive and negative geometry of the cutting wedge with different angle of taking instrument. Mathematical model is the input for experimental verification of the primary contact of milling tool and is aimed at improving the process of milling.

Keywords: primary contact, roughness, cutting forces, face milling.

Analiza pierwszego styku ostrza skrawającego z materiałem obrabianym i jego wpływ na proces frezowania czołowego

Streszczenie

W artykule przedstawiono model matematyczny pierwszego styku ostrza skrawającego z materiałem obrabianym w procesie frezowania czołowego. W opracowaniu modelu uwzględniono narzędzia skrawające o ujemnej i dodatniej geometrii ostrza w różnym położeniu. Uzyskane zależności stanowią podstawę do wykonania doświadczalnej weryfikacji procesu frezowania czołowego z uwzględnieniem wpływu geometrii pierwszego styku ostrza z materiałem obrabianym na parametry wynikowe procesu w celu poprawy jego efektywności.

Słowa kluczowe: obszar pierwszego styku ostrza z materiałem obrabianym, chropowatość, składowe siły skrawania, frezowanie czołowe

1. Introduction

The usage of cutting materials in milling entails some risks connected with their mechanical properties. Milling process is a complex machining method in which a variety of factors are essential. A very important factor is the geometry of the milling tool and its structure, which influences the milling process. Milling process is inherently intermittent continuous section, which puts great demands on the properties such as fracture toughness and flexural strength of a machine tool. It is therefore highly necessary to optimize the right place, in

Address: Prof. J. PILC, Eng. PhD., T. CZÁNOVÁ, Eng., M. SZIGETY, Eng., R. BOBROVSKY, Eng., Department of Machining and Manufacturing Technology, Faculty of Mechanical Engineering, University of Žilina, Univerzitná 8215/1, 010 26 Žilina, Slovakia, jozef.pilc@fstroj.uniza.sk,

which shocks occur. This major place is an input respectively, the primary contact of the tooth cutting tool with the workpiece.

A separate group of milling tools are milling heads, which are produced with large diameters. This is a special group of milling tools with plates of sintered carbides.

2. Geometry of milling heads

In terms of design milling heads have three types of geometry Fig. 1 [1]. Milling heads with negative geometry are suitable for machining steel and cast iron workpieces in mass production. They are designed for heavily cultivated materials and heavy-duty cutting knives. Chip contact length with the front plate is high for materials which make plastic splinter and occurs extortion, choking or cutting groove. Negative geometry is not suitable for heavy duty for milling in broad areas [2].



Fig. 1. Example of milling heads with different geometry [1]

Milling heads with positive geometry are suitable for machining steel and alloy workpieces and wherever power or machine tool is rigidity lower. Chip contact length with the front plate is smaller and can be good for aluminum alloys to form a cutting wedge.

Milling heads with positive and negative geometry are heads allow smooth discharge of long chips when machining steels and alloys of cooper. They are also suitable for iron alloys. In combination with an appropriate angle spiral chips are created cooper, which are well removed from the site of the cut.

The choice of the diameter of milling head is usually made according to the size of the machined area the position of the miller to the workpiece and the type

of contact between the cutting edge and the workpiece. The practice the milling tool diameter is larger 20-50% than the width of the milling area [3÷10].

3. Traction ratios of milling heads

Milling heads are fitted with plates from SK, which do not conform to bending and shock loading, it is therefore necessary to know the conditions of the first image tool with the workpiece. Knowledge of these conditions allows to select geometry tool given the workpiece. Location of primary contact is an area where there is a first contact of face surface of milling tool with the workpiece. The contact of the front tool and workpiece may be in point, line or area. In addition to the type of contact, the relative position of the tool and workpiece is important Fig. 2.

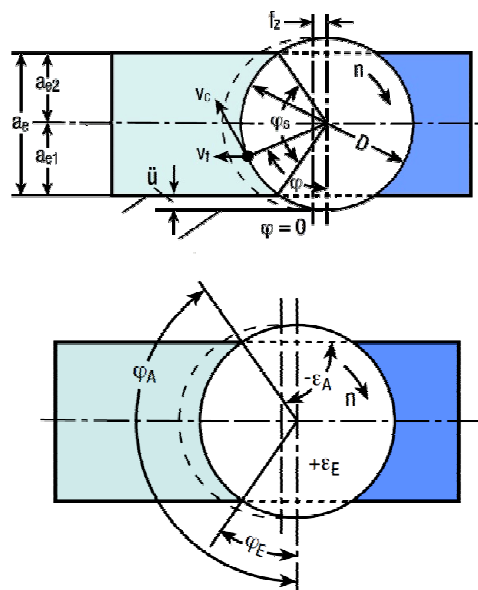


Fig. 2. Contact conditions and geometry in face milling with workpiece [4]

4. The analysis of the place of the primary contact of the milling head

The first point of contact of a milling tool is a very important issue, because it significantly affects the durability of the cutting tool and milling quality in terms of the obtained surface roughness obtained. Roughness is generally

influenced by the shape of the tip and the minor cutting edge. Inappropriate setting, as mentioned above, can be regarded as occupying an area ("STUV"), because already at the first contact creates a full cross section of chips and cutting wedge is subjected to considerable shock Fig. 3.

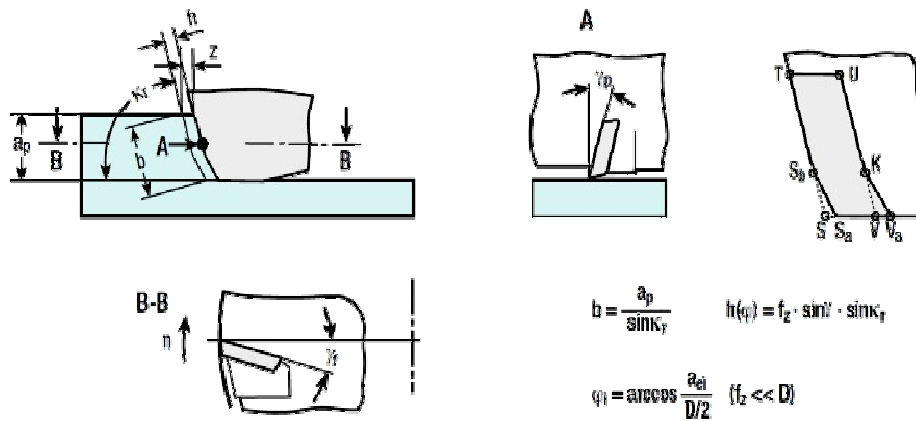


Fig. 3. Contact conditions and cutting edge geometry in face milling [4]

On the other hand should be the primary contact point can be expected as "T". This shot is possible thanks to the appropriate mix of tool geometry and the miller head position relative to the workpiece. It can also be the first contact to point "T", located in the upper part of the active tool. If the value of touch is pointed, we can state that the first touch of the "S" is particularly inappropriate because it is connected with the tip of the plate where there is a danger of fracture due to shock. The contact line between "UV" and "UT", e.g. edge contact outside "delicate" contact with the cutting edge is acceptable. Possible, but not particularly suited is the shot with "SV". It might be said that a decisive influence on the situation has the angle of entry into plane of the workpiece – " ε ", which is the position adjustment tool to the workpiece.

Analytical relations for the determination of contact can be derived from Fig. 4. The figure suggested cutting plate (front plate) and the ground plane Pr. From the figure it is possible to derive the distance of any point "P" face plate from the ground plane. Projection of point "P" to the base plane is the point "R". The front surface of the plate is generally inclined at angles γ_p and γ_f (see Fig. 4). Axis of miller are oriented perpendicular to the work surface. In the analysis we consider that the start-up plane is parallel to the direction of tool feed rate, while parallel to the axis of the milling head.

$$h_t = h[\operatorname{tg}\gamma_p - \operatorname{tg}\psi_r \cdot \operatorname{tg}\gamma_f] + s_z \cdot \operatorname{cose} \cdot \operatorname{tg}\gamma_f \quad (6)$$

Point V is given: $h_p = 0$ $f = f_z \cdot \operatorname{cose}$

$$h_v = h_p \cdot \operatorname{tg}\gamma_p + f \cdot \operatorname{tg}\gamma_f \quad (7)$$

$$h_v = f_z \cdot \operatorname{cose} \cdot \operatorname{tg}\gamma_f \quad (8)$$

In determination of the place of the first contact with the workpiece tool let us assume that start-up plane is parallel to the direction of feed rate and also the axis of the tool. The tracks of teeth are tracks in a circle whose radius is the radius of the tool. Starting arc is very short and the potential diameter tool can be considered linear. This is the only simplification of the analysis. Traction STUV points are arranged in the shape of rhomboid, whose height is equal to the image depth " a_p " and width is equal to feed per tooth " f_z ". Selected point "P" is at the forefront of the rise of the far plane value "y":

$$y = y_s - f \cdot \operatorname{tge} + h_\varepsilon \quad (9)$$

Substituting h_ε from the resulting equation gives the equation, because S-point is located directly in the ground plane (common point and plane P_r and $A\gamma$) point S will accrue on a course:

$$y = y_s \quad (10)$$

The track point T will be applied:

$$y_T = y_s - f \cdot \operatorname{tge} + h_p \cdot \operatorname{tg}\gamma_p + f \cdot \operatorname{tg}\gamma_f \quad (11)$$

when:

$$h_p = h \quad f = -h \cdot \operatorname{tg}\psi_r$$

getting:

$$y_T = y_s + h \cdot \operatorname{tg}\psi_r \cdot \operatorname{tge} + h \cdot \operatorname{tg}\gamma_p - h \cdot \operatorname{tg}\psi_r \cdot \operatorname{tg}\gamma_f \quad (12)$$

and for the appropriate treatment:

$$y_T = y_s - h \cdot [\operatorname{tg}\psi_r \cdot (\operatorname{tg}\gamma_f - \operatorname{tge}) - \operatorname{tg}\gamma_p] \quad (13)$$

Determination of the equation for the track of the "U"

$$y_U = y_S - f \cdot \operatorname{tg} \varepsilon + h_{\varepsilon} \quad (14)$$

point U is given by $h_p = h$

$$f = f_z \cdot \operatorname{cose} - h \cdot \operatorname{tg} \psi_r \quad (15)$$

$$h_{\varepsilon} = h \cdot \operatorname{tg} \gamma_p + (f_z \cdot \operatorname{cose} - h \cdot \operatorname{tg} \psi_r) \cdot \operatorname{tg} \gamma_f \quad (16)$$

$$y_U = y_S - (f_z \cdot \operatorname{cose} - h \cdot \operatorname{tg} \psi_r) \cdot \operatorname{tg} \varepsilon + h \cdot \operatorname{tg} \gamma_p + f_z \cdot \operatorname{cose} \cdot \operatorname{tg} \gamma_f - h \cdot \operatorname{tg} \psi_r \cdot \operatorname{tg} \gamma_f \quad (17)$$

after treatment:

$$y_U = y_S + f_z \cdot \operatorname{cose} \cdot (\operatorname{tg} \gamma_f - \operatorname{tg} \varepsilon) - h \cdot [\operatorname{tg} \psi_r \cdot (\operatorname{tg} \gamma_f - \operatorname{tg} \varepsilon) - \operatorname{tg} \gamma_p] \quad (18)$$

track of point „V“:

$$y_V = y_S - f \cdot \operatorname{tg} \varepsilon + h_{\varepsilon} \quad (19)$$

for point „V“

$$f = f_z \cdot \operatorname{cose} \quad h_p = h = 0 \quad (20)$$

$$h_{\varepsilon} = h_p \cdot \operatorname{tg} \gamma_p + f_z \cdot \operatorname{cose} \cdot \operatorname{tg} \gamma_f \quad (21)$$

after substitution:

$$y_V = y_S - f_z \cdot \operatorname{cose} \cdot \operatorname{tg} \varepsilon + f_z \cdot \operatorname{tg} \gamma_f \cdot \operatorname{cose} \quad (22)$$

$$y_V = y_S + f_z \cdot \operatorname{cose} \cdot (\operatorname{tg} \gamma_f - \operatorname{tg} \varepsilon) \quad (23)$$

substitution phrases:

$$\Delta = h \cdot [\operatorname{tg} \psi_r \cdot (\operatorname{tg} \gamma_f - \operatorname{tg} \varepsilon) - \operatorname{tg} \gamma_p] \quad (24)$$

$$\Theta = f_z \cdot \operatorname{cose} \cdot (\operatorname{tg} \gamma_f - \operatorname{tg} \varepsilon) \quad (25)$$

As mentioned above, there may be the following cases of contact:

- pointed (any of the points STUV),

- bared (at the junction of any two points rhomboid STUV pages),
- surfaced (a surface impact).

Surface shot STUV occurs when (Table 1):

$$y_S = 0, y_T = 0, y_U = 0, y_V = 0 \quad (26)$$

The relationship shows that:

$$\Delta = 0, \Theta = 0 \quad (27)$$

After the substitution, we get:

$$y_T = y_S - \Delta, y_U = y_S - \Delta + \Theta, y_V = y_S + \Theta \quad (28)$$

Table 1. Points surface shot STUV

Shot S occurs if:	Shot T occurs if:	Shot U occurs if:	Shot V occurs if:
$\Delta < 0, \Theta > 0,$ $\gamma_f > ?$	$\Delta > 0, \Theta > 0,$ $\gamma_f > ?$	$\Delta > 0, \Theta < 0,$ $\gamma_f < ?$	$\Delta < 0, \Theta < 0,$ $\gamma_f < ?$

If we consider a linear shot, that may occur at the junction of the following points (Table 2):

$$S - T, U - V, S - V, T - U.$$

Table 2. Points surface shot junction of the following points: S – T, U – V, S – V, T – U

Shot S – T occurs if:	Shot U – V occurs if:	Shot S – V occurs if:	Shot T – U occurs if:
$\Delta = 0, \Theta > 0,$ $\gamma_f > ?$	$\Delta = 0, \Theta < 0,$ $\gamma_f < ?$	$\Delta < 0, \Theta = 0,$ $\gamma_f = ? \quad \gamma_p > 0$	$\Delta > 0, \Theta = 0,$ $\gamma_f = ?, \quad \gamma_p < 0$

5. Procedure measurement of experiments

The experimental part of the measurement was applied to the milling machine type FA 4 AV. The measurements were performed on the test specimen of steel type 11 373, where the first experiment was performed without eccentric displacement e , gradually edged cutter eccentric shift of 5 mm in the positive shift of up to 20 mm and also in the negative direction. Experimental

measurements have been made in applying the cutters with positive and negative geometry, where the number of possible cutting discs was 9, and another measurement was used as a cutting disc for more efficient acquisition and comparison of measured values. Roughness was measured on the device – MAHR PM 30. The measured surface roughness changed from the center of the sample to shift cutter samples as shown in Fig. 5. Measurement of the size of the forces was performed using a piezoelectric dynamometer KISTLER 9255. There were measured three components of the total cutting force F in the direction of the x , y and z . Experimental measurement of cutting conditions with a cutting disc were as follows:

$$v_c = 196,5 \text{ m} \cdot \text{min}^{-1} \quad f_t = 75 \text{ mm} \cdot \text{min}^{-1}$$

$$a_p = \text{const.} = 2 \text{ mm} \quad v_f = f_z \cdot z \cdot n = 0,15 \cdot 1 \cdot 500 = 75 \text{ mm/min}^{-1}.$$

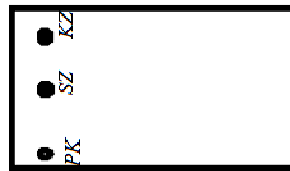
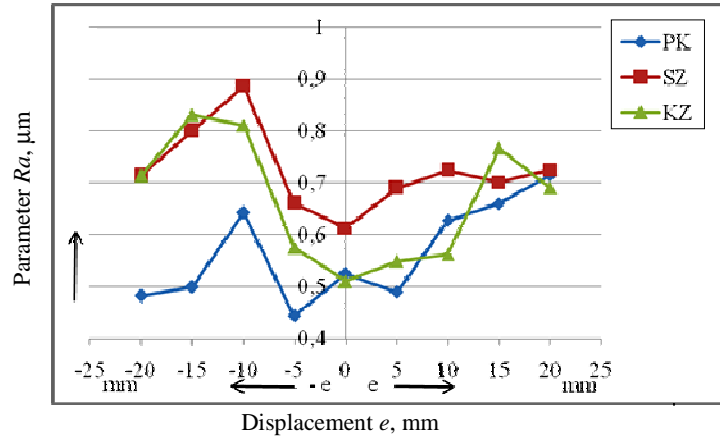


Fig. 5. Position of the measuring points of roughness at the site of primary contact PK, center workpiece SZ and end workpiece KZ

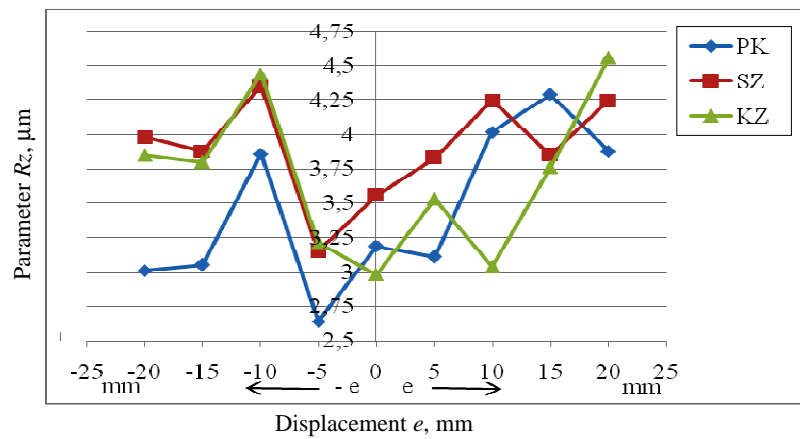
The results of measured roughness R_a and R_z of the negative milling cutter head with one cutting plate (Tab. 3, 4 and Fig. 6, 7).

Table 3. Measurement of surface roughness R_a by milling with negative milling head

Displacement e , mm	Surface Roughness R_a , μm		
	Measure place PK	Measure place SZ	Measure place KZ
-20	0.482	0.714	0.714
-15	0.499	0.801	0.831
-10	0.642	0.886	0.810
-5	0.443	0.661	0.575
0	0.525	0.613	0.510
5	0.489	0.690	0.549
10	0.627	0.724	0.562
15	0.660	0.701	0.767
20	0.715	0.725	0.690

Fig. 6. Surface Roughness R_a and the displacement e Table 4. Measurement of maximum height R_z by milling with negative milling head

Displacement e , mm	Maximum Height Roughness R_z , μm		
	Measure place PK	Measure place SZ	Measure place KZ
-20	3.01	3.98	3.85
-15	3.05	3.88	3.80
-10	3.86	4.35	4.44
-5	2.64	3.15	3.21
0	3.19	3.55	2.98
5	3.11	3.83	3.53
10	4.02	4.25	3.04
15	4.29	3.85	3.76
20	3.88	4.25	4.56

Fig. 7. Maximum height roughness R_z and the displacement e

The results of measured roughness Ra and Rz for the positive milling cutter head with one cutting plate (Tab. 5, 6 and Fig. 8, 9).

Table 5 Measurement of surface roughness Ra by milling with positive milling head

Displacement e , mm	Surface Roughness Ra , μm		
	Measure place PK	Measure place SZ	Measure place KZ
-20	0.873	0.923	0.775
-15	0.673	0.581	0.976
-10	0.745	0.832	0.838
-5	0.713	0.927	0.641
0	0.485	0.4865	0.477
5	0.376	0.547	0.413
10	0.52	0.458	0.536
15	0.607	0.626	1.45
20	0.653	0.662	0.567

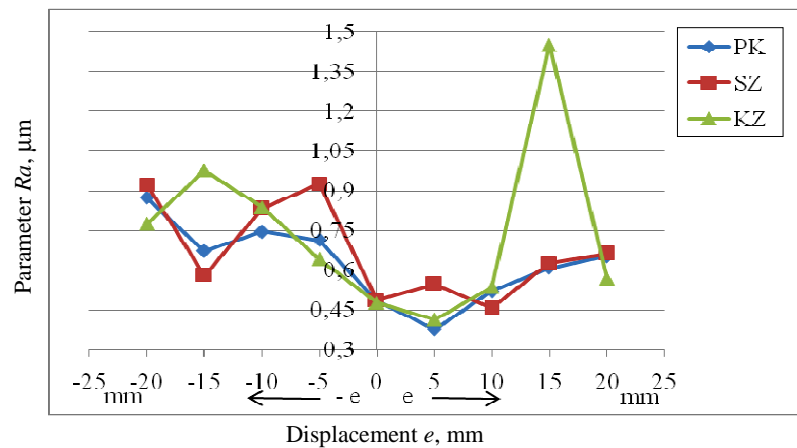


Fig. 8. Surface roughness Ra and the displacement e

Milling single point plate for positive and negative displacement of miller does not have to such a major impact on the change of Ra than with 9 cutting inserts. Ra values were close to each other and do not change so much.

The results of measurements of cutting forces components F_x , F_y and F_z with negative and positive milling cutter head (Tab. 7, 8 and Fig. 10-13).

Table 6. Measurement of maximum height roughness R_z by milling with positive milling head

Displacement e , mm	Surface Roughness R_z , μm		
	Measure place PK	Measure place SZ	Measure place KZ
-20	5.28	4.64	4.77
-15	4.14	4.06	5.42
-10	5.32	5.11	4.96
-5	4.38	5.45	4.86
0	3.285	3.03	2.925
5	2.29	3.71	2.45
10	3.23	3.12	3
15	3.9	4.03	9.18
20	3.86	4.14	3.96

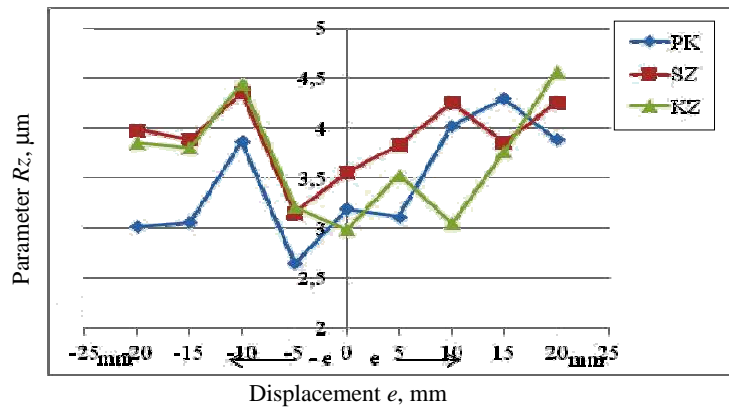


Fig. 9. Maximum Height Roughness R_z and the displacement e

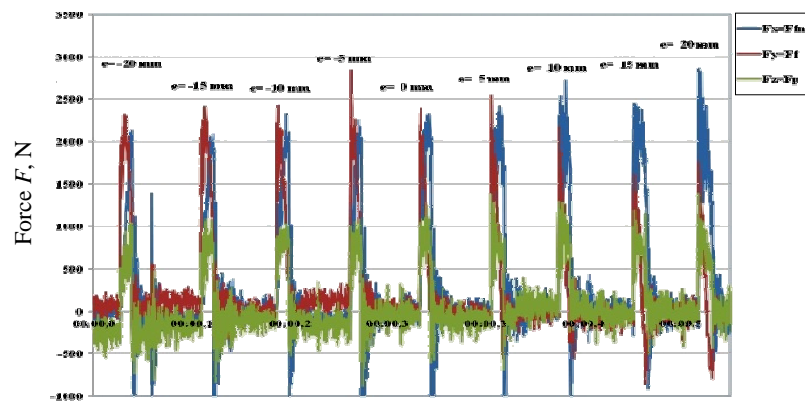


Fig. 10. Course components of cutting forces in application of the negative points of the geometry and the displacement of a tooth

Table 7. The measured values of F_x , F_y , F_z by milling with negative milling cutter head

Displacement e , mm	Force F , N		
	$F_x = F_{f1}$	$F_y = F_f$	$F_z = F_p$
-20	1005	1122	568
-15	1057	1104	579
-10	1070	1078	587
-5	1079	1034	682
0	1094	1043	643.5
5	1105	995	586
10	1118	988	648
15	1162	825	583
20	1220	792	602

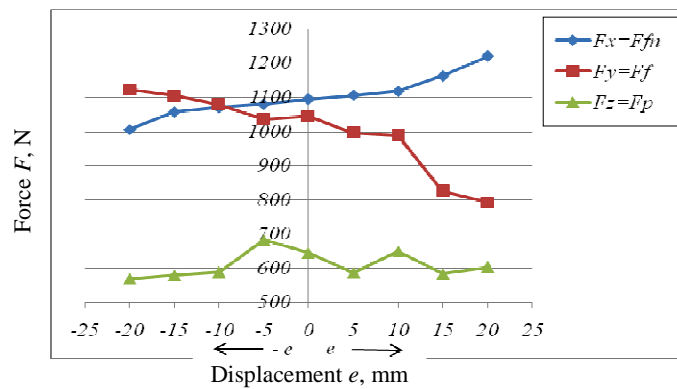
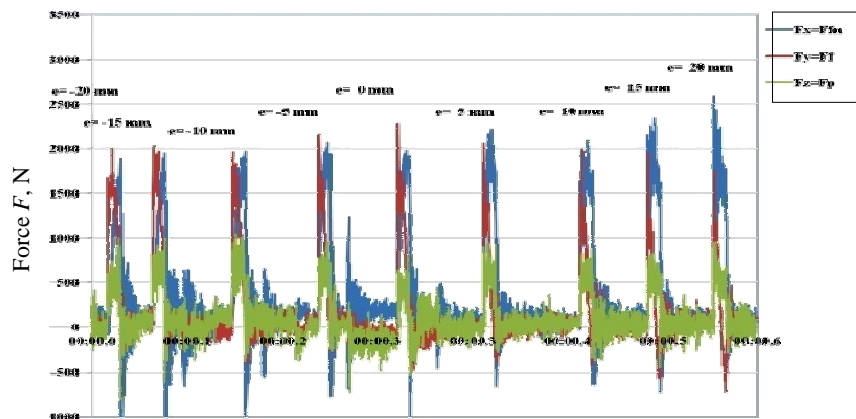
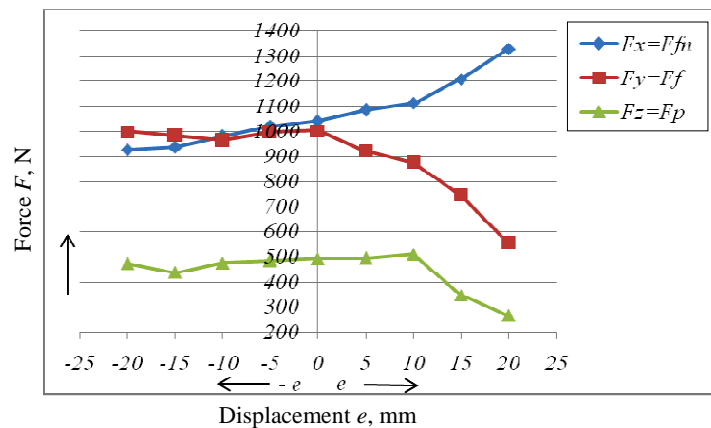
Fig. 11. The arithmetic process of cutting forces components in applications of negative geometry and in points of the displacement e of a toothFig. 12. The arithmetic process of cutting forces components in applications of positive geometry and in points of the displacement e of a tooth

Table 8. The measured values of F_x , F_y and F_z by milling with positive milling cutter head

Displacement e , mm	Force F , N		
	$F_x = F_{fn}$	$F_y = F_f$	$F_z = F_p$
-20	927	998	475
-15	937	983	437
-10	979	964	476
-5	1020	997	485
0	1041,5	1002,5	492,5
5	1084	920	495
10	1112	875	510
15	1207	745	348
20	1328	552	266

Fig. 13. The arithmetic process of cutting forces components in applications to the positive geometry and in points of the displacement e of a tooth

6. Conclusion

There was analyzed the issue of the primary contact for face milling. The experiment was to apply two geometries milling head with a negative primary contact geometry "TU" and a positive geometry of the primary contact "SV". Milling was done to change the position of the eccentric displacement of the plus and minus values of " e ". From the experimental results it can be concluded that changing the position of the tool against the workpiece influence significant changes in quality parameters, such as surface roughness Ra and Rz . It was also observed a significant difference in roughness of the machined surface of the primary and finale image of the cutting tool. The greatest difference was in the values shown in the negative space displacement. The tool was offset by the positive values of the eccentric displacement of surface roughness showed a

steady size in all three measured areas. During the observation of dynamic measurement of cutting forces were recorded appreciable impact forces in tangential and radial direction to the changing course of the size of the forces of change with eccentric displacement e . The negative point values are size of the dynamic displacement components in the radial and tangential direction at approximately the same level. The tool moves to positive values, eccentric take on a tangential force displacement times higher values to the radial forces. Based on the findings can be concluded that the milling head to the workpiece moved into negative territory eccentric displacement " e " will negative affect the life of the instrument itself.

Gradual resolution of the calculation and design elements will also use computer technology to replace some routine operations and simplify the design work. The design tool is based on precise and exact procedures. The quality of the instrument can be improved by using appropriate materials and heat treatment in the event of a hard surface layers. Currently are using tools with mechanical fastening plates of sintered carbides, which are better cutting properties and durability.

References

- [1] <http://www.mcs.sk> [2011-16-02]
- [2] V. UHLÁŘ, I. MRKVICA: Problematika prvního záběru břitu nástroje při frézování. University of Ostrava, Ostrava 2005.
- [3] V. UHLÁŘ, I. MRKVICA: Problematika prvního záběru břitu nástroje při frézování. WORKSHOP fakulty strojní, University of Ostrava, Ostrava 2006.
- [4] W. KÖNIG, F. KLOCKE: Fertigungsverfahren Drehen, Fräsen, Bohren. 8. neu bearbeitete Auflage, Springer-Verlag Berlin, Heidelberg-New York 2008.
- [5] V. UHLÁŘ, I. MRKVICA: Problematika prvního záběru břitu nástroje při frézování. Proc. Conf. Nové trendy vo výrobných technológiách 2006, Prešov 2006.
- [6] J. BUDA, J. SOUČEK, K. VASILKO: Teória obrábania. ALFA: Bratislava 1983.
- [7] <http://www.kvt.sjf.stuba.sk>
- [8] <http://www.matnet.sav.sk/index.php>
- [9] R. ČEP, P. PFEILER, J. PROCHÁZKA, D. STANČEKOVÁ, A. CZÁN: ISCARs ceramic cutting tools testing with an interrupted cut. *Technologické inžinierstvo*, (2009)2.
- [10] N. NÁPRSTKOVÁ, F. HOLEŠOVSKÝ: Admeasurement of grinding wheel loss at FPTM. Proc. 24th International Colloquium Advanced Manufacturing and Repair Technologies in Vehicle Industry, 2007, 159-164.

Received in August 2012